IRSTI 29.05.41 https://doi.org/10.26577/ijmph.20261716

LENSING IMAGES OF DILATONIC BLACK HOLES

Zh.Beisenbekova [1], A.Urazalina [1], M.Khassanov [1], D.Utepova [2] and H.Quevedo [1,3,4]

[1] *Institute for Experimental and Theoretical Physics, Al-Farabi Kazakh National University, Almaty, Kazakhstan*
[2] *Abai Kazakh National Pedagogical University, Almaty, Kazakhstan*
[3] *Instituto de Ciencias Nucleares, Universidad Nacional Autónoma de México, AP 70543, Ciudad de México 04510, Mexico*
[4] *Dipartimento di Fisica and ICRA, Università di Roma "La Sapienza", I-00185 Roma, Italy*

Email: khassanov.manas@kaznu.kz

(Received 15 April 2026; revised 2 May 2026; accepted 13 May 2026)

Abstract. This paper investigates the optical characteristics of a static spherically symmetric dilatonic black hole. The primary objective of the study is to examine the effect of the dilatonic charge Q and the dilaton coupling parameter a on the shadow geometry and the structure of Einstein rings. The research methodology is based on numerical simulations using the backward ray-tracing method, employing the Lagrangian formalism for the photon equations of motion. The main results show that an increase in the dilatonic parameters leads to a significant "compactification" effect of the shadow, the diameter of which can decrease by 31% relative to the Schwarzschild limit at extreme parameter values. Furthermore, a characteristic visual thickening of higher-order photon rings is observed, while maintaining complete topological stability of the image. The scientific value of this work lies in identifying specific optical signatures that allow distinguishing dilatonic black holes from the classical objects of General Relativity. The practical significance of the results is related to their potential application in interpreting observational data from the Event Horizon Telescope (EHT) and searching for manifestations of physics beyond standard models.

Keywords: Dilatonic Black holes, Ray tracing, Lensing images, Shadow geometry

Introduction

Observations by the Event Horizon Telescope Collaboration (EHT), which for the first time captured the image of the shadow of a supermassive black hole in galaxy M87[1], have opened a new era in the study of strong gravitational fields. The black hole shadow represents one of the most informative manifestations of spacetime curvature [2], and its shape and angular size depend on the parameters of the spacetime describing the gravitational field [3]. These observations, together with the measurements by the GRAVITY Collaboration [4] and the detection of gravitational waves [5], provide unique opportunities for testing the general theory of relativity (GR) and its possible extensions [6, 7].

However, an open question remains whether all astrophysical compact objects are fully described by the Schwarzschild or Kerr solutions [8, 9]. In various modified theories of gravity, as well as in models involving scalar fields, alternative solutions of the Einstein equations arise, typically containing additional parameters [10]. A crucial tool for studying such objects is computer modeling of black-hole shadows and lensing images, which allows one to visualize how the metric parameters affect the observed shape and structure of the shadow[11, 12]. One of the most interesting classes of such solutions is represented by dilatonic black holes, which arise in gravitational models containing two (or more) scalar fields together with Abelian gauge fields [13].

The dilaton is a hypothetical scalar field particle that arises naturally in string theory and various models of quantum gravity. In the framework of the model considered here,

the dilatonic field enters the metric via exponential coupling functions between the scalar and electromagnetic fields, giving rise to families of solutions that deviate from the classical Schwarzschild and ReissnerNordström metrics. We investigate the configuration of a dyon-like dilatonic black hole, which possesses both electric and magnetic 'colored' charges[14].

A key characteristic of this spacetime is the dimensionless coupling parameter a ($0 < a \leq 2$), which is determined by the dilatonic coupling vectors λ_i. Depending on the value of a, this solution can describe various physical limits: as $a \to 0$, it reduces to the Schwarzschild solution ; at $a = 1$, it corresponds to the Sen solution; and at $a = 2$ (in the case of collinear coupling vectors), it reproduces the ReissnerNordström metric[14, 15]. In the present work, using the backward ray-tracing method[16, 3], we perform a numerical analysis of the lensed images and shadows of this black hole. This study aims to identify how variations in the parameters Q and a affect the observed shadow structure, thereby visualizing the nonlinear interaction between the gravitational and scalar fields in the strong-field regime.

Materials and Methods

One of the most efficient computational techniques for numerical modeling of lensed images is the backward ray-tracing method, which has been widely used in simulations of black-hole shadows and gravitational lensing images [17]. This approach involves propagating photons backward in timefrom the observer toward the gravitational source. Within this technique, which has been standardized in studies of black hole shadows [18, 19], the dilatonic black hole is placed at the origin of the chosen coordinate system, while the observer is located at the point (r_O, θ_O, ϕ_O). The numerical simulations were performed using a high-performance computing cluster. The technical characteristics of this computational facility are described in [20] A virtual spherical surface is constructed around the black hole, conventionally referred to as the background sphere, which serves as the source of light. Its surface is divided into four regions, each assigned a different colorred, green, yellow, and blue. This color scheme makes it easy to identify the regions from which photons originate after experiencing gravitational deflection.

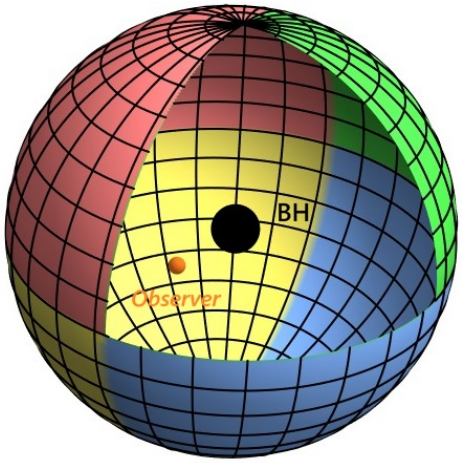

Figure 1 - Schematics of the mapping of Black Hole and observer.

For each pixel in the observers image plane, defined in the observers local coordinate system, the initial conditions for a photon ray are calculated. Each point in the image plane is specified by a pair of coordinates (x_s, y_s), which correspond to the initial propagation direction of the photon. These initial conditions are then transformed into the coordinates of the black hole[18] (r, θ, ϕ)

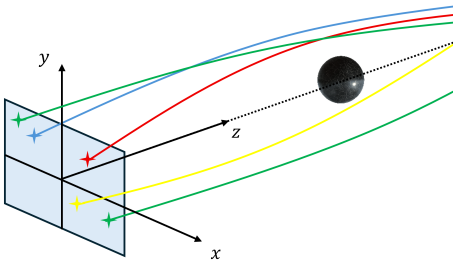

Figure 2 - Geometric projection of the photons in the observers frame.

$$r(0) = \sqrt{r_O^2 + x_s^2 + y_s^2} \tag{1}$$

$$\theta(0) = \cos^{-1}\left(\frac{r_O\cos\theta_O + y\sin\theta_O}{r(0)}\right) \quad (2)$$

$$\phi(0) = \tan^{-1}\left(\frac{\Xi\sin\phi_O - x\cos\phi_O}{\Xi\cos\phi_O - x\sin\phi_O}\right) \quad (3)$$

where the auxiliary variable Ξ is defined as:

$$\Xi = y\cos\theta_O - r_O\sin\theta_O \quad (4)$$

and the initial tangent vector $\dot{\mathbf{x}} \approx (0,0,1)$ is translated into

$$\dot{r}(0) = -\frac{r_O}{r(0)} \quad (5)$$

$$\dot{\theta}(0) = \frac{(x^2+y^2)\cos\theta_O - y r_O\sin\theta_O}{r^2(0)\sqrt{x^2+\Xi^2}} \quad (6)$$

$$\dot{\phi}(0) = \frac{x\sin\theta_O}{x^2+\Xi^2} \quad (7)$$

ensuring the consistency of the observers local coordinate system with the coordinates of black hole.

Dyon-like black hole spacetimes

We consider the line element for a dyon-like black hole presented in [14], which has the following form:

$$ds^2 = H^a\Bigg\{-H^{-2a}\left(1-\frac{2\mu}{r}\right)dt^2 + \frac{dr^2}{1-\frac{2\mu}{r}} + r^2(d\theta^2+\sin^2\theta d\phi^2)\Bigg\}. \quad (8)$$

Here $\mu > 0$ is the extremality parameter, and a is the dilaton field coupling constant and H is the moduli function. The parameters μ and a are related to the gravitational mass M and additional parameter $P > 0$ connected to the net (collective) charge Q of a black hole as follows:

$$M = \mu + \frac{a}{2}P \quad (9)$$

$$P = -\mu + \sqrt{\mu^2 + \frac{1}{2}Q^2}. \quad (10)$$

The function H is defined as :

$$H = 1 + \frac{P}{r}. \quad (11)$$

The line element in its general form is expressed in terms of the parameters a, μ and P, which are not always convenient for realistic analyses of different astrophysical scenarios. Therefore, for practical purposes, it is more suitable to express the metric in terms of the total gravitational mass M and the net charge Q, which is related to the Sen black hole charge as $Q = 2Q_{\text{Sen}}$ and the Reissner–Nordström black-hole charge by the relation $Q = \sqrt{2}Q_{\text{RN}}$. Taking into account Eqs. (9) and (10) on can express μ and P in terms of M and Q:

$$\mu = \frac{M}{1-a}\left[1 - \frac{a}{2}\left(1+\sqrt{1+\frac{1-a}{2M^2}Q^2}\right)\right], \quad (12)$$

$$P = -\frac{M}{1-a}\left(1-\sqrt{1+\frac{1-a}{2M^2}Q^2}\right).$$

Introducing a new notation $\Delta = \sqrt{2M^2+(1-a)Q^2}$ we rewrite the line element in terms of the parameters M and Q:

$$ds^2 = -\frac{B}{A^a}dt^2 + \frac{A^a}{B}dr^2 + A^a r^2\left(d\theta^2+\sin^2\theta\, d\phi^2\right) \quad (13)$$

where

$$A = 1 - \frac{2M-\sqrt{2}\Delta}{2(1-a)r}, \quad (14)$$

$$B = 1 - \frac{2(2-a)M-\sqrt{2}a\Delta}{2(1-a)r}.$$

In particular cases, this metric naturally reduces to well-known solutions of general relativity. For example, when $a = 0$ we obtain the

Schwarzschild solution, when $a = 1$ the line element becomes equivalent to the Sen solution and when $a = 2$ it reduces to the ReissnerNordström solution. The relation between the parameter a and the dilaton coupling constant, as well as the physical interpretation of the charge Q in the context of color charges, is discussed in detail in [14, 15, 21, 22, 23].

Simulation and Lensing Images

To construct the lensing images of the dyon-like dilatonic black hole, we numerically integrate the null geodesic equations describing light propagation in the curved spacetime defined by the metric (13). The general form of the geodesic equations for a photon is given as follows:

$$\frac{d^2x^\mu}{d\lambda^2} + \Gamma^\mu_{\alpha\beta}\frac{dx^\alpha}{d\lambda}\frac{dx^\beta}{d\lambda} = 0 \qquad (15)$$

where λ is the affine parameter and $\Gamma^\mu_{\alpha\beta}$ are the Christoffel symbols.For the numerical simulation, we employ the Lagrangian formalism, expressing the equations of motion as a system of explicit second-order ordinary differential equations. Due to the stationarity and spherical symmetry of the solution, the trajectories of the light rays are characterized by two fundamental constants of motion: the energy E and the axial angular momentum L. Utilizing these integrals of motion allows us to obtain a reduced system of equations. In our backward ray-tracing scheme, the specific values of E and L are unique to each ray and are determined by the initial conditions

$$E = H(r(0))^{-a/2}\sqrt{1 - \frac{2\mu}{r(0)}} \qquad (16)$$

$$L = \dot{\phi}(0)r(0)^2\sin^2\theta(0)\cdot H(r(0))^a \qquad (17)$$

where $r(0)$, $\dot{\phi}(0)$, and $\theta(0)$ are given by Eqs. (1–7) and are functions of the observer's screen pixel coordinates (x_s, y_s).

The explicit form of the reduced equations of motion, as well as the expressions for all non-zero Christoffel symbols, are provided in Appendix A.

We present the gravitational lensing images and shadows of a dilatonic black hole obtained via numerical backward ray-tracing simulations. The observer is placed at a finite distance $r_O = 15M$, while the black-hole mass is normalized to $M = 1$. The observers image plane is defined in the local Cartesian coordinates $x_s \in [-13, 13]$ and $y_s \in [-13, 13]$ spanning the ranges.

The resulting simulated images, illustrating the influence of the charge Q and the dilaton parameter a on the black hole shadow and the surrounding lensing rings, are presented in Fig. 3.

Results and Discussion

This section presents the results of numerical simulations of shadows and gravitational lensing for a static spherically symmetric dilatonic black hole. Particular attention is paid to the effect of the dilatonic charge Q and the dilaton coupling parameter a on the optical properties of the spacetime described by metric (8) and (13).

Maintaining spherical symmetry and the Schwarzschild limit

As can be seen from the obtained images, for all investigated values of the parameters Q and a, the black hole shadow maintains a perfectly circular shape. The circular symmetry of the shadow was verified numerically, allowing its size to be characterized by a single parameter the diameter measured in the 1000×1000 computational grid. (see Table 1). This result is in full agreement with the static nature of the investigated metric.

An important step in validating our model is the behavior of the system at a. Image analysis has shown that $a = 0$, the apparent diameter of the shadow remains constant (≈ 382 grid units) regardless of the value of the dilatonic charge Q (verified for $Q = 0.5$, 1.0, and 1.414). Mathematically, this is explained by the fact

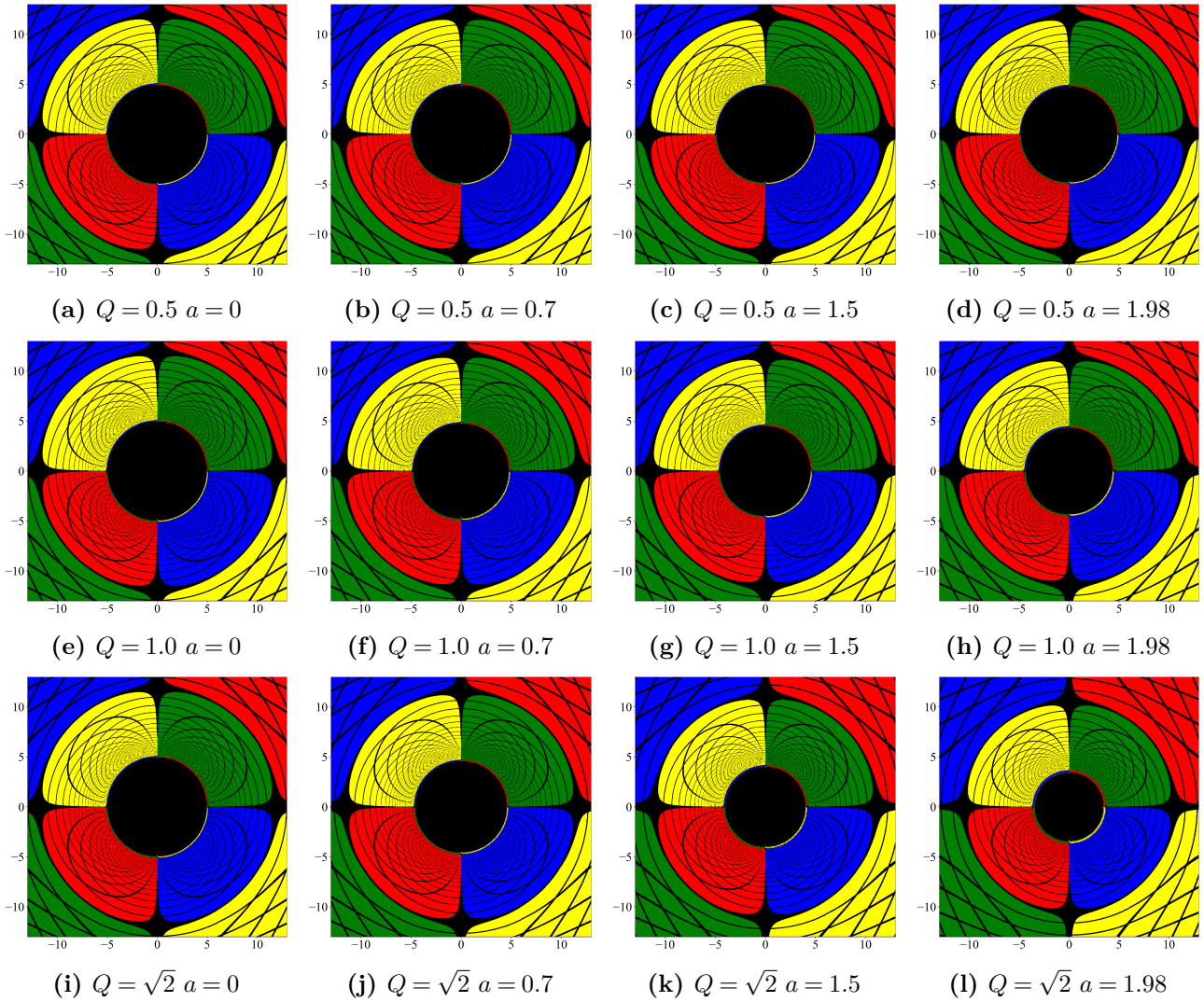

(a) $Q = 0.5$ $a = 0$ **(b)** $Q = 0.5$ $a = 0.7$ **(c)** $Q = 0.5$ $a = 1.5$ **(d)** $Q = 0.5$ $a = 1.98$

(e) $Q = 1.0$ $a = 0$ **(f)** $Q = 1.0$ $a = 0.7$ **(g)** $Q = 1.0$ $a = 1.5$ **(h)** $Q = 1.0$ $a = 1.98$

(i) $Q = \sqrt{2}$ $a = 0$ **(j)** $Q = \sqrt{2}$ $a = 0.7$ **(k)** $Q = \sqrt{2}$ $a = 1.5$ **(l)** $Q = \sqrt{2}$ $a = 1.98$

Figure 3 - Gravitational lensing images and shadows of a dilatonic black hole obtained via backward ray tracing for different values of the electric charge Q and the dilaton coupling parameter a. (a)(l).

that the structural function H^a degenerates to unity, and the metric reduces to the classical Schwarzschild solution. Thus, the parameter Q has no independent effect on the radius of the photon sphere without the inclusion of the dilaton coupling a.

Compactification of the shadow under the influence of the dilaton field

The main distinguishing feature of the investigated dilatonic black hole is the strong effect of nonlinear "compactification" of the shadow. The inclusion of the dilaton field leads to a decrease in the critical impact parameter of photons. We conducted a rigorous analysis of the shadow sizes across the entire set of 12 simulations. The average diameter is defined as the mean value of the shadow size measured along the horizontal and vertical directions. The relative size is expressed as a percentage with respect to the Schwarzschild case ($a = 0$), which is taken as the reference value (100%). All other configurations are normalized to this baseline, the results of which are presented in table 1.

The obtained results indicate that the parameters Q and a act synergistically, with a serving as a pronounced exponential amplifier of the compactification effect. At a weak charge ($Q = 0.5$), an extreme increase of

Table 1 – The dependence of the shadow's geometric properties on the dilaton charge Q and the coupling parameter a

(Q)	(a)	average diameter in 1000Œ1000 grid	Relative size (%)
0.5	0	≈ 382	100.0
0.5	0.7	≈ 378	99.1
0.5	1.5	≈ 374	98.0
0.5	1.98	≈ 371	97.4
1.0	0	≈ 382	100.0
1.0	0.7	≈ 368	96.4
1.0	1.5	≈ 348	91.1
1.0	1.98	≈ 334	88.0
1.414	0	≈ 382	100.0
1.414	0.7	≈ 352	92.3
1.414	1.5	≈ 309	80.9
1.414	1.98	≈ 266	69.3

a to 1.98 shrinks the shadow by only 2.6%. However, at the maximum investigated charge ($Q = 1.414$), the transition to strong coupling ($a = 1.98$) leads to a radical drop in the capture cross-section areathe apparent diameter of the shadow decreases by almost $\approx 30\%$ relative to the Schwarzschild case. This demonstrates the extreme sensitivity of the photon sphere geometry to the combined influence of the scalar and electromagnetic fields.

Einstein ring structure and horizon stability

In addition to the size of the shadow, the dilaton parameters significantly influence the optical structure of spacetime in the vicinity of the black hole. At large values of Q and a, the coordinate grid lines become visually sparser at a distance from the shadow, whereas the structure of the photon rings (higher-order images), conversely, becomes noticeably thicker and broader. A strong dilaton field specifically modifies the divergence behavior of the light deflection angle, preventing the secondary images of the celestial sphere from exponentially compressing into an infinitely thin contour. As a result, the optical rings near the photon sphere become visually wider and more pronounced. It is important to note that, unlike the q-metric for naked singularities [11]where the Einstein ring disintegrates into chaotic pseudo-ringsthe dilaton solution demonstrates absolute topological stability. In all considered configurations, the Einstein ring remains continuous, confirming the preservation of the event horizon.

Conclusions

In this study, numerical modeling of shadows and gravitational lensing for a static dilaton black hole was performed using the backward ray-tracing method. The primary focus was placed on analyzing the influence of the dilaton charge Q and the coupling parameter a on the observable characteristics of the photon sphere.The quantitative analysis revealed a strong nonlinear "compactification" effect of the black hole shadow. It was found that at large values of the dilaton charge, the coupling parameter a acts as an exponential amplifier, significantly reducing the critical impact parameter of photons. In the extreme cases ($Q = 1.414$, $a = 1.98$), a reduction in the apparent diameter of the shadow by 31% compared to the Schwarzschild limit was recorded. At the same time, the topology of the Einstein rings remains stable, indicating the presence of an event horizon and the absence of pathological artifacts (pseudo-rings or regions of repulsive gravity) inherent to naked singularities.The obtained results have implications for interpreting observational astrophysics data. In light of the observations by the Event Horizon Telescope (EHT) collaboration, one of the primary tasks is to search for deviations of real compact objects from the predictions of classical General Relativity (GR). Our study demonstrates that a dilaton black hole can appear up to 30% "smaller" than a Schwarzschild black hole of the same mass. If independent dynamical measurements of a compact object's mass (e.g., via the kinematics of the accretion disk) yield a specific value, but the observed shadow size turns out to be systemati-

cally smaller than the expected theoretical radius, this could serve as a strong observational signature for the presence of a dilaton field. Our results demonstrate that the characteristics of compact object shadows can serve as an observational probe for testing gravity and other field theories in the strong-field regime, which until recently remained inaccessible to observation.

Acknowledgment

This research is funded by the Science Committee of the Ministry of Science and Higher Education of the Republic of Kazakhstan (Grant No. AP26195301, Principal Investigator: Dr. Manas Khassanov).

Appendices

In this appendix, we provide the explicit expressions for the non-vanishing Christoffel symbols $\Gamma^{\mu}_{\alpha\beta}$ associated with the static spherically symmetric dilatonic metric defined in Eq. (15), as well as the corresponding equations of motion. We adopt the standard coordinates $x^{\mu} = (t, r, \theta, \phi)$.

$$\Gamma^{t}{}_{tr} = \Gamma^{t}{}_{rt} = \frac{2(a-2)M + \sqrt{2}\,a\Delta}{2r\left[2(a-1)r - 2(a-2)M - \sqrt{2}\,a\Delta\right]},$$

$$\Gamma^{r}{}_{tt} = \frac{2(a-2)M + \sqrt{2}\,a\Delta}{8(a-1)^2 r^3} \times \left(2(a-1)r - (a-2)M + \sqrt{2}\,a\Delta\right) \times \left(1 + \frac{2M - \sqrt{2}\Delta}{2(a-1)r}\right)^{-2a},$$

$$\Gamma^{r}{}_{rr} = -\frac{2(a-2)M + \sqrt{2}\,a\Delta}{2r\left[2(a-1)r - 2(a-2)M - \sqrt{2}\,a\Delta\right]},$$

$$\Gamma^{r}{}_{\theta\theta} = \frac{2(a-2)M + \sqrt{2}\,a\Delta}{2(a-1)} - r,$$

$$\Gamma^{r}{}_{\phi\phi} = -\left(\frac{2(a-2)M + \sqrt{2}\,a\Delta}{2(a-1)} - r\right)\sin^2\theta,$$

$$\Gamma^{\theta}{}_{r\theta} = \Gamma^{\theta}{}_{\theta r} = \frac{1}{r},$$

$$\Gamma^{\theta}{}_{\phi\phi} = -\cos\theta\sin\theta,$$

$$\Gamma^{\phi}{}_{r\phi} = \Gamma^{\phi}{}_{\phi r} = \frac{1}{r},$$

$$\Gamma^{\phi}{}_{\phi\theta} = \Gamma^{\phi}{}_{\theta\phi} = \cot\theta,$$

where $\Delta = \sqrt{2M^2 + (1-a)\,Q^2}$.

$$\dot{\phi} = \frac{L\csc^2\theta}{r^2}\left(1 + \frac{2M - \Delta}{2(a-1)r}\right)^{-a},$$

$$\ddot{\theta} = \frac{L^2\cot^2\theta\csc^2\theta}{r^4}\left(1 + \frac{2M - \sqrt{2}\,\Delta}{2(a-1)r}\right)^{-2a} - \frac{4(a-1)r - (a-2)\left(2M - \sqrt{2}\,\Delta\right)}{r\left(2M - \sqrt{2}\,\Delta + 2(a-1)r\right)}\,\dot{r}\,\dot{\theta},$$

$$\ddot{r} = \alpha + \beta - \gamma + \delta$$

where

$$\alpha = \frac{L^2\csc^2\theta\left(1 + \frac{2M - \sqrt{2}\,\Delta}{2(a-1)r}\right)^{-2a}}{4r^4\left(2M - \sqrt{2}\,\Delta + 2(a-1)r\right)} \times (a-1)\left[(2M - \sqrt{2}\,\Delta) - 4r\right] \times \left[2M + \sqrt{2}\,\Delta - 2r\right],$$

$$\beta = \frac{(a-1)E^2}{r\left(2M - \sqrt{2}\,\Delta + 2(a-1)r\right)} \times \frac{\left[-4M^2 + a(a-1)Q^2 + 2\sqrt{2}\,M\Delta - 4(a-1)Mr\right]}{\left(2(a-1)r - 2(a-2)M - \sqrt{2}\,a\Delta\right)},$$

$$\gamma = \frac{\alpha_2}{E^2}\,\dot{r}^2,$$

$$\delta = \frac{\left[(a-2)(2M - \sqrt{2}\Delta) - 4(a-1)r\right]}{4(a-1)\left(2M - \sqrt{2}\Delta + 2(a-1)r\right)} \times \left[2(a-2)M + \sqrt{2}\,a\Delta - 2(a-1)r\right]\dot{\theta}^2.$$

Author Contributions: Conceptualization, A.U. and M.K.; methodology, M.K., D.U.; software, Zh.B., M.K.; validation, A.U.; formal analysis, D.U.; investigation, Zh.B., A.U., and D.U.; resources, Zh.B.; data curation, Zh.B.; writingoriginal draft preparation, M.K., A.U., D.U. and Zh.B.; writingreview and editing, M.K.; visualization, Zh.B.; supervision, A.U., H.Q.; project administration, M.K. All authors have read and agreed to the published version of the manuscript.

References

[1] Event Horizon Telescope Collaboration, K. Akiyama *et al.* "First M87 Event Horizon Telescope Results. I. The Shadow of the Supermassive Black Hole." 875, no. 1 (2019): L1.

[2] Cunningham, C. T. and J. M. Bardeen. "The Optical Appearance of a Star Orbiting an Extreme Kerr Black Hole." 183 (1973): 237–264.

[3] Luminet, J. P. "Image of a Spherical Black Hole with Thin Accretion Disk." 75 (1979): 228–235.

[4] Abuter, R., A. Amorim, N. Anugu, M. Bauböck, M. Benisty, J. P. Berger, N. Blind, H. Bonnet, W. Brandner, A. Buron, others, and T. G. Collaboration. "Detection of the gravitational redshift in the orbit of the star S2 near the Galactic Centre massive black hole." *Astronomy & Astrophysics* 615 (2018): L15.

[5] Abbott, B. P., LIGO Scientific Collaboration, and Virgo Collaboration. "Observation of Gravitational Waves from a Binary Black Hole Merger." 116, no. 6 (2016): 061102.

[6] Will, C. M. "The Confrontation between General Relativity and Experiment." *Living Reviews in Relativity* 17 (2014): 4.

[7] Berti, E., C. Bambi, P. C. C. Freire, C. Lämmerzahl, D. Psaltis, and J. Sauer. "Probing modified gravity with the Event Horizon Telescope." *Physical Review D* 92 (2015): 124047.

[8] Shaikh, R., P. Kocherlakota, R. Narayan, and P. S. Joshi. "Shadows of spherically symmetric black holes and naked singularities." *Monthly Notices of the Royal Astronomical Society* 482, no. 1 (2018): 52–64.

[9] Bambi, C. "X-ray tests of general relativity with black holes." *Symmetry* 15, no. 6 (2023): 1277.

[10] Stephani, H., D. Kramer, M. A. H. MacCallum, C. Hoenselaers, and E. Herlt. *Exact Solutions of the Einstein Field Equations*. Cambridge: Cambridge University Press, 2003.

[11] Arrieta-Villamizar, J. A., J. M. Velásquez-Cadavid, O. M. Pimentel, F. D. Lora-Clavijo, and A. C. Gutiérrez-Piñeres. "Shadows around the q-metric." *Classical and Quantum Gravity* 38, no. 1 (2020): 015008. https://arxiv.org/abs/2007.13600

[12] Beissen, A., N. S. Utepova, D. N. Kossov, V. S. Toktarbay, K. Khassanov, M. T. Yernazarov, and K. Imanbayeva, A. "Comparing the efficiency of gpu and cpu in gravitational lensing simulation." *International Journal of Mathematics and Physics* 15, no. 1 (2024): 49–56. https://doi.org/10.26577/ijmph.2024v15i1a6

[13] Abishev, M., K. Boshkayev, and V. Ivashchuk. "Dilatonic dyon-like black hole solutions in the model with two abelian gauge fields." *The European Physical Journal C* 77, no. 3 (2017): 180.

[14] Malybayev, A., K. Boshkayev, and V. Ivashchuk. "Quasinormal modes in the field of a dyon-like dilatonic black hole." *The European Physical Journal C* 81, no. 5 (2021): 475.

[15] Boshkayev, K., G. Suliyeva, V. Ivashchuk, and A. Urazalina. "Circular geodesics in the field of double-charged dilatonic black holes." *The European Physical Journal C* 84, no. 1 (2024): 19.

[16] Bardeen, J. M. *et al.* "Timelike and null geodesics in the kerr metric." *Black holes (Les astres occlus)* (1973): 215–239.

[17] Toktarbay, S., N. Beissen, M. Khassanov, A. Muratkhan, A. Orazymbet, A. Sadu, and N. Shynggyskhan. "Exploring the impact of anisotropy parameters on stellar structure." *International Journal of Mathematics and Physics* 16, no. 2 (2025): 4–11.

[18] Lin, F.-L., A. Patel, and H.-Y. Pu. "Black hole shadow with soft hairs." *Journal of High Energy Physics* 2022, no. 9 (2022): 117.

[19] Velásquez-Cadavid, J., J. Arrieta-Villamizar, F. Lora-Clavijo, O. Pimentel, and J. Osorio-Vargas. "Osiris: a new code for ray tracing around compact objects." *The European Physical Journal C* 82, no. 2 (2022): 103.

[20] Vaidman, N. L., A. S. Miroshnichenko, S. V. Zharikov, S. A. Khokhlov, A. T. Agishev, and B. S. Yermekbayev. "Fundamental parameters and evolutionary scenario of hd 327083." *Galaxies* 13, no. 3 (2025): 47.

[21] Sen, A. "Rotating charged black hole solution in heterotic string theory." 69, no. 7 (1992): 1006–1009. 10.1103/PhysRevLett.69.1006

[22] Boshkayev, K. and M. Muccino. "Constraints on the Sen black hole mass and charge from quasi-periodic oscillations." *European Physical Journal C* 85, no. 12 (2025): 1477.

[23] Belissarova, F. B., K. A. Boshkayev, V. D. Ivashchuk, and A. N. Malybayev, "Special dyon-like black hole solution in the model with two Abelian gauge fields and two scalar fields." in *Journal of Physics Conference Series*, ser. Journal of Physics Conference Series, 1690. IOP, Dec. 2020, 012143.

Information about authors

Zhuldyz Beisenbekova – *M.Sc., Al-Farabi Kazakh National University, Almaty, Kazakhstan, e-mail: tanatarova.0398@bk.ru*
Ainur Urazalina – *PhD, Associate Professor, Al-Farabi Kazakh National University, Almaty, Kazakhstan, e-mail: y.a.a.707@mail.ru*
Manas Khassanov – *PhD, Senior lecturer, Al-Farabi Kazakh National University, Almaty, Kazakhstan, e-mail: khassanov.manas@kaznu.kz*
Daniya Utepova – *PhD, Acting Associate Professor, Abai Kazakh National Pedagogical University, Almaty, Kazakhstan, e-mail: utepova_daniya@mail.ru*
Hernando Quevedo – *Full Professor and Researcher, Instituto de Ciencias Nucleares, Universidad Nacional Autónoma de México, AP 70543, Ciudad de México 04510, Mexico, e-mail: quevedo@nucleares.unam.mx*